not, in general, entered into his control problems. This classical separation of the three fields of analysis has led to a general lack of understanding, coordination, and communication between aeroelasticians and flight control analysts. This is, indeed, unfortunate. These people are all working on the same problem area and, if you will, the same equations of motion—the major difference being the frequency range of interest. Aeroelasticians are interested primarily in the higher frequencies and flight control analysts in low frequency and rigid-body dynamics. It is also unfortunate that separate departments have been set up by most companies to deal with the two areas; this has served to widen the technical communication gap.

In the very near future, as advanced vehicles become more flexible, the flutter-type dynamics are going to present problems in the design of the flight control system. The increased structural flexibility will require control system bandwidths of operation to be increased while the elastic mode frequencies are tending downward, with the result that the pure flutter dynamics may feed energy into the control system dynamics as well as the vehicle rigid-body modes. This could result in an extremely complex three-way coupling problem. To effectively cope with this type of situation, it is imperative that aeroelasticians, stability and control analysts, and flight control analysts mount their attack of the problem on a more common analysis ground than exists between the three groups today. An important first step in this direction would be for companies and agencies to merge these people into truly unified dynamic analysis departments.

References

[1] Swaim, R. L., "Effect of low-frequency elastic mode shape on forward-loop stability characteristics of winged boosters," Air Force Flight Dynamics Lab. ASRMCM-TM-62-8 (July 1962).

[2] Swaim, R. L., "Closed-loop stability of a winged-payload booster subject to variations of an elastic mode shape," Air Force Flight Dynamics Lab. ASRMCM-TM-62-11 (November 1962).

[3] Swaim, R. L., "Further investigation of elastic mode effects on closed-loop stability of a winged booster," Air Force Flight Dynamics Lab. ASRMCM-TM-63-1 (April 1963).

Planar-Wound Filamentary Pressure Vessels

R. F. HARTUNG*
Lockheed Missiles and Space Company, Palo Alto, Calif.

FIGURE 1 depicts a dome with base radius R suitable for the end closure of a pressure vessel and formed by winding resin-coated high-strength filaments onto a mandrel and then heat-treating the resulting structure to produce a hard and resistant composite. The filaments are deposited along lines defined by the intersection of the surface with a plane making an angle γ with the axis of revolution z. Such a winding pattern leads to what will be referred to as a planar-wound filamentary structure. It is further assumed that the filaments are always deposited in pairs that are symmetric with respect to a meridian.

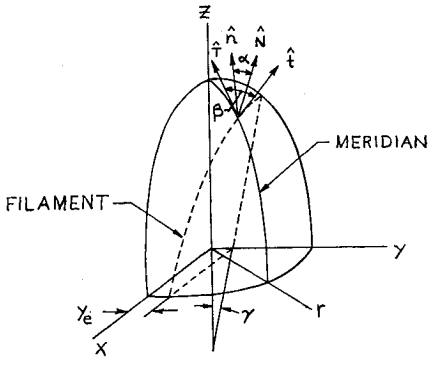

Fig. 1 Typical planar-wound dome and associated geometry.

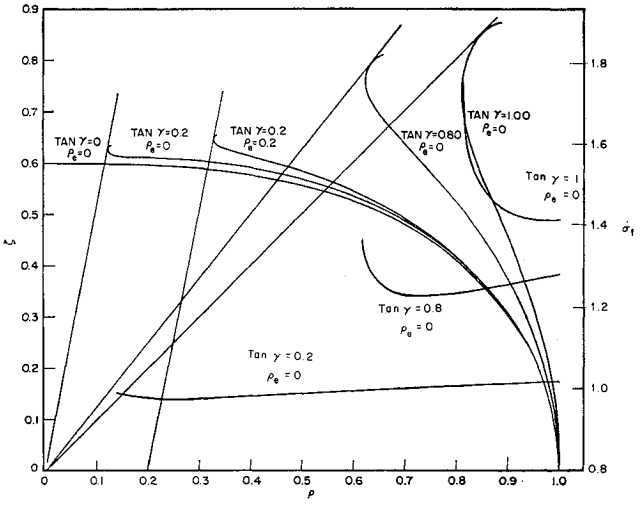

Fig. 2 Balanced design planar-wound dome contours and associated stresses.

If the dome meridian curve is defined by

$$r = r(z) \tag{1}$$

then the principal radii of curvature in the meridional and circumferential directions, respectively, are

$$r_1 = -(1 + r'^2)^{3/2}/r'' \qquad r_2 = r(1 + r'^2)^{1/2} \tag{2}$$

where primes denote differentiation with respect to z. For a closed dome in equilibrium under the action of uniform pressure p and in the absence of axial load, the meridional and circumferential stress resultants are, respectively,†

$$N_\phi = pr_2/2 \qquad N_\phi = (pr_2/2)[2 - (r_2/r_1)] \tag{3}$$

Projection of the filament curve on the (y,z) plane gives

$$x^2 = r^2 - (y_e + z\tan\gamma)^2 \tag{4}$$

y_e is defined in Fig. 1. An expression for the winding angle β between the meridian curve and filament curve is obtained from the definition

$$\cos\beta = \hat{t}\cdot\hat{T} \tag{5}$$

$\hat{T}$ and $\hat{t}$ being the unit tangent vectors of the meridian and filament curves, respectively. Combining (4) and (5), one obtains

$$\tan^2\beta = \frac{[\rho\dot{\rho} - (\rho_e + \zeta\tan\gamma)\tan\gamma]^2 + (\tan^2\gamma - \dot{\rho}^2)[\rho^2 - (\rho_e + \zeta\tan\gamma)^2]}{(1 + \dot{\rho}^2)[\rho^2 - (\rho_e + \zeta\tan\gamma)^2]} \tag{6}$$

where

$$\rho = \frac{r}{R} \qquad \zeta = \frac{z}{R} \qquad \rho_e = \frac{y_e}{R} \qquad (\dot{}) = \frac{d(\ )}{d\zeta}$$

Presented at the AIAA Launch and Space Vehicle Shell Structures Conference, Palm Springs, Calif., April 1–3, 1963; revision received September 12, 1963.

* Member, Mechanical and Mathematical Sciences Laboratory.

† Limitations on the use of (3) for orthotropic shells are discussed in Ref. 1.

Because the filaments will not generally lie along geodesics on the shell surface, there will be a tendency for them to slip. The angle α between the normal to the surface $\hat{N}$ and the normal to the filament $\hat{n}$ may be taken as a measure of this tendency. For planar-wound domes, the definition $\cos\alpha = \hat{N}\cdot\hat{n}$, together with Eq. (4), yields

$$\cos\alpha \frac{[\rho^2 - (\rho_e + \zeta\tan\gamma)^2]\sec\gamma + [(\rho_e + \zeta\tan\gamma)\sin\gamma + \rho\dot{\rho}\cos\gamma][\rho\ddot{\rho} - (\rho_e + \zeta\tan\gamma)\tan\gamma]}{\rho(1+\dot{\rho}^2)^{1/2}\{[\rho\dot{\rho} - (\rho_e + \zeta\tan\gamma)\tan\gamma]^2 + \sec^2\gamma[\rho^2 - (\rho_e + \zeta\tan\gamma)^2]\}^{1/2}} \tag{7}$$

By considering the equilibrium of an element of the shell and assuming compatibility in strain between the filaments and filler material, Hoffman[2] has obtained the following expressions for the stresses in the filaments σ_f and in the filler $\sigma_{m\theta}, \sigma_{m\phi}, \tau_{\max}$:

$$\sigma_f = \frac{N_\theta(\sin^2\beta - \nu_m\cos^2\beta) + N_\phi(\cos^2\beta - \nu_m\sin^2\beta)}{2D} \tag{8a}$$

$$D = h_f(\sin^4\beta + \cos^4\beta - 2\nu_m\sin^2\beta\cos^2\beta) + (h_m E_m/2E_f)$$

$$\sigma_{\theta m} = \frac{N_\theta[(h_f/h_m)\cos^2\beta(\cos^2\beta - \nu_m\sin^2\beta) + (E_m/2E_f)] - N_\phi[(h_f/h_m)\sin^2\beta(\cos^2\beta - \nu_m\sin^2\beta)]}{D} \tag{8b}$$

$$\sigma_{\phi m} = \frac{-N_\theta[(h_f/h_m)\cos^2\beta(\sin^2\beta - \nu_m\cos^2\beta)] + N_\phi[(h_f/h_m)\sin^2\beta(\sin^2\beta - \nu_m\cos^2\beta) + (E_m/2E_f)]}{D} \tag{8c}$$

$$\tau_{\max} = \frac{-N_\theta[(h_f/h_m)(1-\nu_m)\cos^2\beta + (E_m/2E_f)] + N_\phi[(h_f/h_m)(1-\nu_m)\sin^2\beta + (E_m/2E_f)]}{2D} \tag{8d}$$

where E is the modulus of elasticity, ν is Poisson's ratio, and subscripts f and m refer to the filament and filler, respectively. The net filler thickness h_m is given by

$$h_m = h - 2h_f$$

h being the total thickness of the shell composite and h_f the equivalent filament thickness defined by

$$h_f = A/d = nA/2\pi r\cos\beta \tag{9}$$

$2A$ represents the cross-sectional area of the filaments forming one filament pair and d the perpendicular distance between successive filaments; h_f then represents the thickness of an equivalent solid sheet of filament material.

The final part of Eq. (9) is obtained by assuming that each filament crosses all parallel circles on the dome an equal number of times (i.e., filaments do not terminate or double back); n is the number of equal segments into which the parallel circles are divided by the intersecting filaments. In addition to this primary state of filler stress given by Eqs. (8b–8d), a secondary stress state is generated by changes in the filaments force along the filament centerline and the tendency of the filament to slip out of the winding plane. Only the primary stresses are considered in this note.

The stress analysis of a planar-wound dome of arbitrary meridian proceeds as follows. Given the meridian curve (1) and the winding parameters γ and ρ_e, the angle β is computed using (6). Having β, and selecting appropriate values for E_m, E_f, ν_m, A, and n, the stresses in the filaments are computed from (8a–8d).

Concept of Balanced Design

The membrane solution for a planar-wound dome has been formulated assuming that both filler and filaments are available to carry the loads. The conditions under which a filler material of zero strength ($E_m = 0$, $\nu_m = 0$) can be used are now examined. If the filler has no strength, it must not be subjected to stresses.‡ Equating (8b–8d) to zero leads to the requirement that

$$\tan^2\beta = N_\theta/N_\phi \tag{10}$$

Equation (10) is referred to as the condition of balanced design. Setting $E_m = \nu_m = 0$ in (8a) and substituting (10) for $\sin^2\beta$ yields

$$\sigma_f = N_\phi/2h_f\cos^2\beta \tag{11}$$

Appropriate combination of (2, 3, 10, and 11) leads to the following set of three equations in four unknowns σ_f, β, h_f, and $\rho(\zeta)$:

$$\sigma_f = \frac{\rho(1+\dot{\rho}^2)^{1/2}pR}{h_f\cos^2\beta\,4} \tag{12}$$

$$\tan^2\beta = 2 + \frac{\rho\ddot{\rho}}{1+\dot{\rho}^2} \tag{13}$$

$$h_f = \frac{nA}{2\pi R}\frac{1}{\rho\cos\beta} \tag{14}$$

To this system one must add either (1) or (5) but not both. Thus, for balanced design, if a meridian curve is specified, there is no freedom as to the choice of the filament pattern, whereas, if the filament pattern is specified, the meridian shape will no longer be arbitrary.

Planar-Wound Balanced Design Profiles

The differential equation for the meridian curve of a planar-wound dome with balanced design is obtained by combining (6) and (10) to obtain

$$[\rho\dot{\rho} - (\rho_e + \zeta\tan\gamma)\tan\gamma]^2 = [2 - \tan^2\gamma + \rho\ddot{\rho} + 3\dot{\rho}^2][\rho^2 - (\rho_e + \zeta\tan\gamma)^2] \tag{15}$$

with boundary conditions

$$\rho = 1 \text{ and } \dot{\rho} = 0 \text{ at } \zeta = 0 \tag{16}$$

An exact solution to (15) could not be obtained, and so, using numerical techniques, meridian curves were obtained for various values of ρ_e and γ. These are plotted in Fig. 2. For the special case of $\rho_e = 0$, these results agree with those obtained by Mueller.[3]

An expression for the filament stress associated with these profiles is obtained from (12, 14, and 6):

$$\sigma_f = \frac{p\pi R^2}{2nA}\rho^2 \times \left\{\frac{[\rho\dot{\rho} - (\rho_e + \zeta\tan\gamma)\tan\gamma]^2 + \sec^2\gamma[\rho^2 - (\rho_e + \zeta\tan\gamma)^2]}{\rho^2 - (\rho_e + \zeta\tan\gamma)^2}\right\}^{1/2} \tag{17}$$

‡ Secondary filler stresses mentioned earlier are again ignored.

References

[1] Hartung, R. F., "Membrane analysis of filament wound structures," AIAA Preprint 2915-63 (April 1963).

[2] Hoffman, O., "Analysis of filament-wound pressure vessels," Lockheed Missiles and Space Co. LMSD-480823, Sunnyvale, Calif. (May 1960).
[3] Mueller, F. M., "Some theoretical developments on the analysis of filament-wound vessels," Lockheed Aircraft Corp. Rept. 15137, Burbank, Calif. (April 1960).

Decay of a Magnetohydrodynamic Shock Wave Produced by a Piston

Roy M. Gundersen*
The University of Wisconsin-Milwaukee, Milwaukee, Wis.

It is the purpose of this note to discuss the interaction of a uniform shock wave and a centered rarefaction wave in the one-dimensional, unsteady flow of an ideal, inviscid, perfectly conducting, monatomic, compressible fluid subjected to a transverse magnetic field. Let a uniform shock wave be generated by pushing a piston with constant velocity into a tube filled with gas at rest, and, at some later time, let the piston be stopped abruptly thus generating a centered rarefaction wave, which propagates with true-sonic speed and ultimately overtakes the shock and diminishes its strength. Under the assumption that the shock wave is weak or at most of moderate strength, the width of the interaction zone and the subsequent motion of the shock wave may be determined by the use of the author's extension[1] of the Friedrichs' theory[2, 3] for conventional gasdynamic flows. For a monatomic fluid, generalized Riemann invariants[4] and the flow parameters in a centered simple wave[5] may be determined explicitly. These facts form the basis for a simple extension of the Friedrichs' theory to the magnetic case, and, in the limit of vanishing magnetic field, the extended theory reduces exactly to that derived by Friedrichs.

Let u, c, B, μ, ρ, $b^2 = B^2/\mu\rho$, $\omega = (b^2 + c^2)^{1/2}$, $\Omega = u + \omega$, $m = b/c$, and U be, respectively, the particle velocity, local speed of sound, magnetic induction, permeability, density, square of the Alfvén speed, the true-sonic speed, slope of the forward-facing characteristics of the simple wave, a measure of the applied field, and shock velocity. Let the flow in front of the shock be denoted by the subscript zero, and let the subscript one denote the flow behind the shock or in front of the rarefaction wave. Consequently, the velocity of the piston is u_1, and the shock velocity is U_1. Further, it is assumed that the piston is stopped at time t_R at the position $x_R = u_1 t_R$.

For the magnetic case, the generalized Riemann invariants are[4]

$$u/2 + (\omega/c)^3/k = \alpha$$
$$-u/2 + (\omega/c)^3/k = \beta$$

where k is constant, and the Friedrichs' theory assumes $\beta_0 = (\omega_0/c_0)^3/k$ remains constant across the shock, i.e., the shock transition is replaced by the transition through the corresponding compression simple wave.

The strength of the shock may be characterized by the function $\sigma(\xi)$, defined by $\Omega - \omega_0 = \omega_0\sigma(\xi)$, where ξ is a parameter constant along a rectilinear characteristic of the simple wave. For a monatomic fluid, u and ω may be determined explicitly in terms of Ω, and, in particular, since ω_1 may be expressed in terms of u_1, the piston velocity, it suffices to state that

$$\sigma_1 = [u_1 + \omega_1(u_1) - \omega_0]/\omega_0 \tag{1}$$

which is known. Then the shock velocity may be determined from the formula[1]

$$U_1 = \omega_0[1 + \sigma_1/2 + D\sigma_1^2/8] \tag{2}$$

where

$$D = [69m_1^4 + 136m_1^2 + 64 - 4m_1^2(1 + m_1^2)^{3/2}]/(8 + 9m_1^2)^2$$

and

$$\lim_{m_1 \to 0} D = 1$$

The centered rarefaction wave may be described by $x = x_R + \Omega(t - t_R)$, and its strength is determined by the condition that the flow behind it, characterized by the subscript two, is at rest. Consequently, $u_2 = 0$, and it follows that $\sigma_2 = 0$ and $\omega_2 = \omega_0$, so that the motion of the tail of the rarefaction wave is given by

$$x = x_T = x_R + \omega_0(t - t_R)$$

The head of the rarefaction wave catches up with the shock at a time t_1 at a position

$$x_1 = U_1 t_1 = x_R + (u_1 + \omega_1)(t_1 - t_R) \tag{3}$$

From Eqs. (1–3), it follows that

$$t_1 = 8\omega_1 t_R/\omega_0\sigma_1(4 - D\sigma_1)$$

The solution for the shock path obtained when a weak shock interacts with a rarefaction wave described by

$$x = \xi + \Omega(\xi)t$$
$$\Omega(\xi) = u(\xi) + \omega(\xi)$$
$$-u(\xi)/2 + [\omega(\xi)/c(\xi)]^3/k = \beta_0$$

is given by

$$\omega_0 t(\xi) = 8\left[\frac{4 - D\sigma_1(\xi)}{\sigma_1(\xi)}\right]^2 \int_\xi^0 \frac{\sigma_1(y)dy}{[4 - D\sigma_1(y)]^3} \tag{4}$$

In order to use Eq. (4) for the present problem in which the interaction begins at $t = t_1$, it is convenient to describe the simple wave with respect to a new origin (x_1, t_1). This gives

$$x - x_1 = \omega_0(1 + \sigma)(t - t_1) + \omega_0(t_1 - t_R)(\sigma - \sigma_1) \tag{5}$$

From Eq. (5), it follows that $\xi = -\omega_0(t_1 - t_R)(\sigma_1 - \sigma)$, and substituting into Eq. (4), which is the magnetohydrodynamic generalization of Eq. (8.6) of Ref. 2, the following result is obtained:

$$t \equiv t_s = t_1 + \frac{8(t_1 - t_R)}{\sigma^2(4 - D\sigma_1)^2}[\sigma^2(D\sigma_1 - 2) - D\sigma_1^2\sigma + 2\sigma_1^2] \tag{6}$$

Therefore,

$$x \equiv x_s = x_R + \omega_0(1 + \sigma)(t - t_R) \tag{7}$$

Equations (6–7) give the parametric representation of the motion of the shock. In order to describe this motion by giving x as a function of t, Eq. (6) may be inverted to give $\sigma = \sigma(t)$ which, upon substitution into Eq. (7), gives $x = x(t)$. From the asymptotic form of this result, valid for large t and consequently for small σ, it may be seen, exactly as in the conventional gasdynamic case, that the width of the decaying shock wave, i.e., the distance between the shock front and the tail of the rarefaction wave, increases in direct proportion to the square root of the time elapsed.

Received June 17, 1963.
* Professor of Mathematics.

References

[1] Gundersen, R. M., "Linearized analysis of one-dimensional magnetohydrodynamic flows," *Springer Tracts in Natural Philosophy* (Springer-Verlag, Berlin, to be published), Chap. 6.
[2] Friedrichs, K. O., "Formation and decay of shock waves," Commun. Pure Appl. Math. 1, 211–245 (1948).